

Charge Dynamics Across the Disorder Driven Superconductor-Insulator Transition

Sabyasachi Tarat and Pinaki Majumdar

Harish-Chandra Research Institute, Chhatnag Road, Jhusi, Allahabad 211019, India

(Dated: September 27, 2022)

While insensitive to weak non magnetic disorder, an s -wave superconductor can be driven insulating by strong disorder. Using a scheme that captures the correct ground state, and fully retains thermal amplitude and phase fluctuations, we describe the disorder driven superconductor-insulator transition at finite temperature. Our results on the resistivity suggest that beyond moderate disorder the low temperature superconducting state can arise out of an ‘insulating’ normal state. We also find that the low frequency weight in the density of states and optical conductivity are non monotonic in disorder, with a maximum near critical disorder, and their high temperature value correlate with the superconducting fraction in the disordered ground state.

The disorder driven superconductor-insulator transition (SIT) is a longstanding problem in condensed matter physics. Although early theoretical work by Anderson [1] suggested that superconductivity (SC) should be insensitive to non-magnetic disorder, a large number of experiments over the last couple of decades [2] have revealed that superconductivity is actually suppressed and finally destroyed by increasing disorder. Simultaneously, the normal state resistivity changes from metallic to insulating, and a pseudogap (PG) appears in the single particle density of states.

The availability of high resolution scanning tunneling spectroscopy (STS) tools has led to a significant advance in the field. Recent observations include: (i) The increasing fragmentation of the SC state with disorder [3–10]. (ii) Survival of an apparent (pseudo)gap in the disorder driven normal state [3–6]. (iii) A change in the temperature dependence of the normal state resistivity from metallic to insulating, without necessarily any universal temperature independent value at critical disorder [11, 12]. Additionally, (iv) there are observations of non monotonic magnetoresistance [12–14], and finite frequency superfluid stiffness at large disorder [15, 16], well past the SIT.

The fully self-consistent Hartee-Fock-Bogoliubov-de Gennes (HFBdG) approach [17] had already revealed that the strong disorder SC ground state is fragmented in an essential way, and predicted the survival of a single particle gap across the SIT. Thermal effects have been probed using quantum Monte Carlo (QMC) [18–20], providing an estimate of T_c and the global density of states. Surprisingly, apart from an early estimate [19], there seem to be no results on the charge dynamics, *i.e.*, the resistivity and optical features, across what is essentially a transport transition. The limitation stems from the inability to handle thermal fluctuations on a large spatial scale, and access real frequency information.

In this paper we solve this problem using an approach that captures the HFBdG ground state, fully retains the thermal amplitude and phase fluctuations, and locates the correct disorder scale, V_c , for the zero temperature SIT.

Our main results, at intermediate coupling, are the following: (i) For $V \ll V_c$ the single particle gap closes at T_c , but beyond $V \sim 0.25V_c$ there emerges a pseudogap window above T_c , and when $V > 0.75V_c$ a *hard gap* persists for $T > T_c$. (ii) The normal state resistivity $\rho(T)$ is ‘insulating’, with $d\rho/dT < 0$, already at $V \sim 0.5V_c$ so, for $0.5V_c < V < V_c$ one actually observes an *insulator to superconductor* transition on cooling the system. (iii) Increasing temperature leads to a growth in the low frequency single particle and optical weight across T_c , over a window $\delta T \ll T_c$ at weak disorder and $\delta T \gtrsim T_c$ at strong disorder. The $T \gg T_c$ weight correlates closely with the ‘superconducting fraction’ in the ground state. (iv) Increasing disorder leads to *non monotonic* behaviour of the low frequency single particle and optical weight, with a peak around $V_c(T)$.

While there is already experimental evidence for (i) and (ii), the other predictions can be tested experimentally and correlated with spatial data where available.

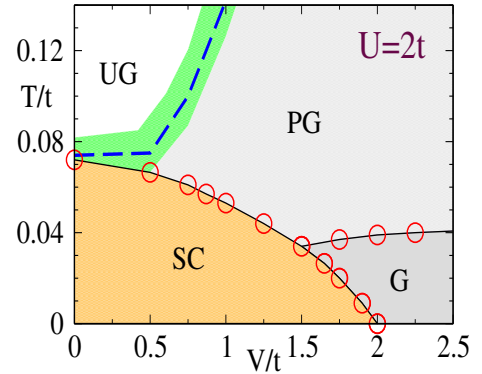


FIG. 1. Colour online: Phase diagram for $U = 2t$ showing the superconducting (SC), and the following non superconducting phases: gapped (G), ungapped (UG) and pseudogapped (PG). The $T = 0$ SIT is at $V_c \sim 2t$. A normal state pseudogap shows up for $V \gtrsim 0.25V_c$ and for $V \gtrsim 0.75V_c$ the $T \gtrsim T_c$ phase actually has a hard gap. The crossover between pseudogapped and notionally ungapped phase is shown by the green area. The blue dashed line shows the transition from an ‘insulating’ ($d\rho/dT < 0$) to ‘metallic’ regime, which lies within the broad crossover.

Model and method: We study the attractive Hubbard model in two dimensions (2D), with disorder incorporated in the form of a random potential V_i at each site.

$$H = H_{kin} + \sum_{i\sigma} (V_i - \mu)n_{i\sigma} - |U| \sum_i n_{i\uparrow}n_{i\downarrow} \quad (1)$$

where $H_{kin} = -t \sum_{\langle ij \rangle \sigma} c_{i\sigma}^\dagger c_{j\sigma}$. $t = 1$ denotes the nearest neighbour tunneling amplitude, U is the strength of on-site attraction, and μ the chemical potential, set so that the electron density is $n \approx 0.9$. The disorder V_i is chosen from a box normalised distribution between $\pm V/2$. We focus on the disorder dependence at $U = 2t$ for specific results and discuss the U dependence at the end.

We rewrite the interaction in terms of auxiliary ‘pairing’ and ‘density’ fields via a Hubbard-Stratonovich (HS) decomposition [21, 22], and choose coefficients to recover HFBdG theory at $T = 0$. We work in the static limit of the auxiliary fields,

$$H_{eff} = H_{kin} + \sum_{i\sigma} (V_i - \mu)n_{i\sigma} + H_{coup} + H_{cl} \quad (2)$$

where $H_{coup} = \sum_i (\Delta_i c_{i\uparrow}^\dagger c_{i\downarrow}^\dagger + h.c.) + \sum_i \phi_i n_i$ and $H_{cl} = (1/U) \sum_i (|\Delta_i|^2 + \phi_i^2)$. The presence of the field ϕ is important, especially in disordered systems, since it captures the enhancement of disorder due to interaction effects.

Unlike mean field theory, we *do not minimise* the free energy with respect to Δ_i and ϕ_i at finite temperature, T , but sample all configurations according to their Boltzmann weight $P\{\Delta, \phi\} \propto Tr_{c, c^\dagger} e^{-\beta H_{eff}}$. The difficulty in this approach is of course in evaluating the weight for an arbitrary configuration. This is handled using the Metropolis algorithm combined with a diagonalisation of the effective Bogoliubov-de Gennes (BdG) problem [23, 24]. We use an $\mathcal{O}(N)$ cluster based scheme [25] for the Monte Carlo updates and can readily access system sizes $\sim 24 \times 24$. Our method captures the HFBdG ground state as $T \rightarrow 0$, since the Δ_i and ϕ_i minimise the free energy in that case, but captures the crucial amplitude and phase fluctuations at finite temperature. We have focused on $U = 2t$, which is the weakest interaction we can controllably access with our system size. Even at $U = 2t$ the gap to T_c ratio in the clean limit is already outside the BCS window. Our results are averaged over at least 10 copies of disorder.

Phase diagram: We begin with the $V - T$ phase diagram in Fig.1, detailing the different phases in terms of transport and spectral character. In the absence of disorder SC order is lost at $T_c = T_c^0 \sim 0.07t$, benchmarked with QMC results [26]. T_c falls below our measurement resolution, $\sim 0.05tT_c^0$, at $V \sim 2t$ and we set this as V_c . T_c^0 and V_c will set the natural scales of temperature and disorder for us. Our observations are the following.

(i) At weak disorder the fractional suppression of T_c is small, *e.g.* at $V = 0.25V_c$, T_c falls less than 10% from T_c^0 . This is qualitatively consistent with the ‘insensitivity’ to disorder predicted by Anderson [1], but that approach fails to be useful beyond weak disorder. We are not aware of analytic results on the suppression of T_c in this coupling regime, although there are numerical results on the reduction of the phase stiffness [17]. Overall, the weak disorder regime, $0 < V < 0.25V_c$, corresponds to almost homogeneous $|\Delta_i|$ in the ground state, metallic resistivity above T_c , and no significant anomaly in the normal state density of states (DOS).

(ii) The intermediate disorder window, $0.25V_c < V < 0.75V_c$, resists easy characterisation. $|\Delta_i|$ in the ground state shows increasing fragmentation [17, 27]. The resistivity is ‘insulating’ near T_c and crosses over to metallic behaviour at high T , while the $T > T_c$ density of states shows a pseudogap.

(iii) At strong disorder, $V \gtrsim 0.75V_c$, the pairing amplitude $|\Delta_i|$ is very inhomogeneous in the ground state, a hard gap survives in the DOS even above T_c , and the resistivity shows activated behaviour. This is a regime where the low T superconducting state emerges from a high T *insulating* phase, suggesting that the T_c is no longer controlled by the low energy DOS.

The different phase boundaries would depend on U/t . Apart from the change in T_c^0 and $V_c(T = 0)$, increasing U/t would lead to an increase in the ‘gapped’ region, while decreasing U/t would decrease the gapped window in favour of the PG (and the UG to PG crossover could be pushed to larger V/V_c).

Resistivity: The resistivity $\rho(T)$ is computed using the Kubo formula, via the low frequency limit of the optical conductivity $\sigma(\omega)$. Formally $\sigma(\omega) = -\omega^{-1} Im(\Lambda_{xx}(q = 0, \omega))$ where the current-current correlation function is defined by

$$\Lambda_{xx}(q = 0, \omega) = \frac{1}{Z} \sum_{n,m} |\langle n | j_{xx} | m \rangle|^2 \frac{e^{-\beta E_n} - e^{-\beta E_m}}{\omega + E_n - E_m + i\delta}$$

The $|n\rangle, |m\rangle$ are many particle eigenstates of the system, j_{xx} is the current operator. For the regular part, $\sigma_{reg}(\omega)$, *i.e.* excluding the superfluid response, it simplifies within our static auxiliary field theory to:

$$\begin{aligned} \sigma_{reg}(\omega) = & \sum_{a,b} F_1(a,b) \frac{(n(\epsilon_a) + n(\epsilon_b) - 1)}{\epsilon_a + \epsilon_b} \delta(\omega - \epsilon_a - \epsilon_b) \\ & + \sum_{a,b} F_2(a,b) \frac{(n(\epsilon_a) - n(\epsilon_b))}{\epsilon_a - \epsilon_b} \delta(\omega - \epsilon_b + \epsilon_a) \end{aligned}$$

where, now, the $\epsilon_\alpha, \epsilon_\beta > 0$, *etc.* are *single particle eigenvalues* of the BdG equations, the $n(\epsilon_\alpha)$, *etc.*, are Fermi functions, and the F ’s are current matrix elements computed from the BdG eigenfunctions. The dc resistivity is defined for $T > T_c$ via $\rho^{-1} = \omega_0^{-1} \int_0^{\omega_0} \sigma_{reg}(\omega) d\omega$, where $\omega_0 \sim 0.1t$.

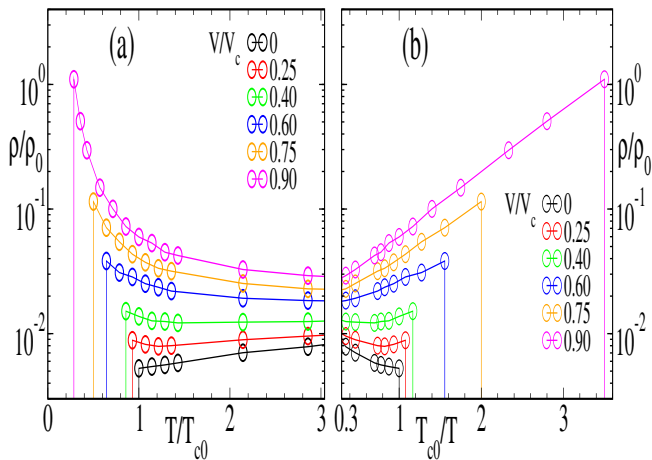


FIG. 2. The resistivity, $\rho(T)$, measured in units of $\rho_0 = \hbar/(\pi e^2)$, evolving from metallic to insulating behaviour in the normal state with growing disorder. For $V \lesssim 0.25V_c$, it is metallic, between $0.25V_c \lesssim V \lesssim 0.75V_c$, it is mixed, showing a thermal transition from ‘insulating’ at low T to weakly ‘metallic’ at larger T . Beyond $V = 0.75V_c$, the low T behaviour is exponential $\rho(T) \propto e^{\Delta_g/T}$, with Δ_g increasing with V . This is highlighted in (b), where we see that such a fit ceases to be valid below $V \sim 0.75V_c$.

Fig.2.(a) shows $\rho(T)$ for different V . We use $d\rho/dT > 0$ to indicate a metal and $d\rho/dT < 0$ to indicate an insulator. Upto $V \sim 0.25V_c$ the resistivity is metallic at all T , except very near T_c . For $0.25V_c < V < 0.75V_c$, however, the behaviour is mixed, with ‘metallic’ character at high T and an ‘insulating’ window below. As the companion plot, Fig.2.(b), shows the weakly insulating behaviour cannot be characterised by a T independent gap in the DOS. Beyond $0.75V_c$ the resistivity is insulating at all T , we have checked it upto $T = 0.3t$. The log plot in Fig.2.(b) shows that the resistivity can be modeled as $\rho(T) \propto e^{\Delta_g/T}$, with a weakly disorder dependent coefficient A and an activation scale $\Delta_g \sim 2.5(V - 0.75V_c)$.

The large disorder regime admits a simple explanation in terms of the current paths. The low energy excitations are localised in the superconducting clusters that form at $T = 0$. Since the SC regions are ‘disconnected’ at $T > T_c$ all current paths have to pass partly through the insulating matrix, leading to an activation factor in the conductance. At weaker disorder the SC clusters have a tenuous connection and the detailed frequency dependence of the DOS is important.

Overall, we observe that for our chosen $U = 2t$, superconductivity can arise out of a metallic or an insulating normal state. Our calculation does not hint at any ‘universal’ temperature independent resistance at $V = V_c$, apparently consistent with recent experimental analysis [13].

Density of states: Fig.3 shows the variation in the single particle DOS with disorder and temperature. If ϵ_n and $\{u_n^i, v_n^i\}$ are the positive BdG eigenvalues and eigen-

vectors, respectively, in some equilibrium configuration, the DOS is computed as

$$N(\omega) = \left\langle \sum_{i,n} |u_n^i|^2 \delta(\omega - \epsilon_n) + |v_n^i|^2 \delta(\omega + \epsilon_n) \right\rangle$$

where the angular brackets indicate thermal average.

In Fig.3.(a) we show the DOS plots at $T = 0$ for varying disorder, from $V = 0$ to $V = 1.5V_c$. The following features are noteworthy. (i) The system is gapped for all V . The ‘gap’ shows a non-monotonic character, decreasing upto $V \sim V_c$ and increasing from thereon. These results match well with previous BdG [17] and QMC [20] benchmarks. (ii) The coherence peaks decrease with increasing V , and beyond $V \sim 0.75V_c$ they are hard to discern in the DOS. The ‘rise’ of the DOS at the gap edge is ideally sharp in the clean limit, corresponding to the square root BCS singularity, but for $V \gtrsim 0.75V_c$ the rise is much gentler.

Fig.3(b) shows the thermal evolution at $V = 0.5V_c$, intermediate disorder, while 3(c) shows the same at $V = V_c$. For $V = 0.5V_c$ the coherence peak at the gap edge vanishes at $T \sim T_c \approx 0.8T_c^0$, the low frequency DOS grows steadily with increasing temperature, but a pseudogap feature survives upto $T \sim 2.5T_c$. 3.(c) shows the result at $V = V_c$, where the system retains a hard gap

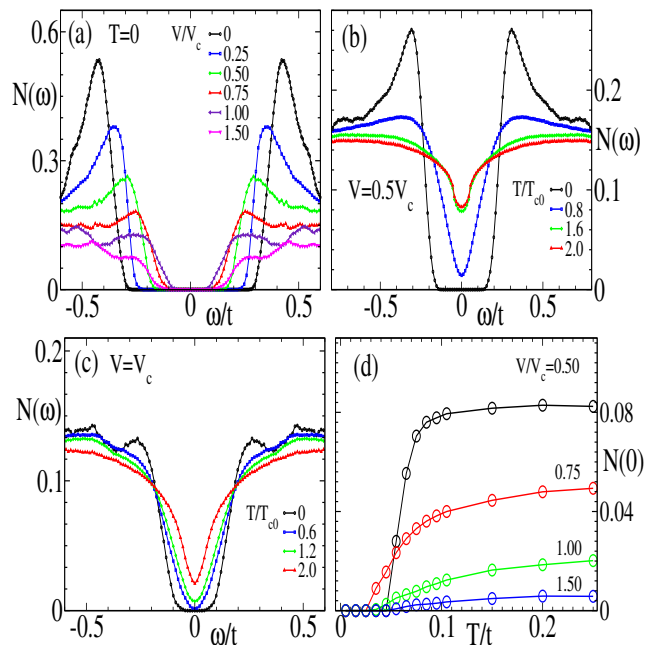


FIG. 3. Colour online: Density of states at $U = 2$. (a). The DOS at low temperature, showing the persistence of a gap at all V , while the coherence peaks are difficult to discern beyond $V \sim 0.75V_c$. (b). Temperature dependence of the DOS for $V = 0.5V_c$, already showing a noticeable pseudogap for $T > T_c$. (c). Same as (b) but for $V \sim V_c$, where the system is insulating at all temperature. (d). Temperature dependence of $N(0)$, the DOS at the Fermi level, for different disorder.

with increasing temperature till $T \sim 0.5T_c^0$ and a deep pseudogap thereafter.

Fig.3.(d) shows the temperature dependence of $N(0)$, the DOS at the Fermi level, for a few V . At $V = 0.5V_c$, $N(0)$ is essentially zero till $T \sim T_c$ and then rises quickly and saturates to a high T asymptote. With growing disorder the temperature interval $\delta T(V)$ over which the rise occurs increases and the ‘asymptotic’ high temperature value reduces. We find that this high temperature value at a given disorder roughly corresponds to the superconducting fraction in the ground state [27] at that disorder.

Optics: Fig.4.(a)-(c) shows aspects of the optical conductivity at two representative temperatures for various V , while 4.(d) shows the integrated low frequency weight as increasing disorder drives the SIT.

In a disordered superconductor, the real part of the optical conductivity consists of a delta function at $\omega = 0$ (signifying dissipationless transport) and a ‘regular’ part $\sigma_{reg}(\omega)$. Within a mean field picture, $\sigma_{reg}(\omega)$ at $T = 0$ is suppressed for $\omega \lesssim 2\Delta$, the gap scale. Beyond this σ_{reg} rises to a peak and for $\omega \gg \Delta$ tends to the disordered metal limit, $\Gamma/(\omega^2 + \Gamma^2)$, where Γ is the scattering rate. Fig.4(a) shows the low T result at different V , consistent with this general expectation. The low V curves have a gap, rise to a relatively sharp maximum and then fall off. Increasing V increases Γ making the fall off broader. In what follows we use just $\sigma(\omega)$ rather than $\sigma_{reg}(\omega)$ to denote the regular part.

It is useful to compare these results with that of Mattis-Bardeen (MB) theory [28], which is formulated in the weak coupling limit. Qualitatively, within MB theory the thermal excitation of quasiparticles to the gap edge, with a probability $\sim e^{-\Delta(T)/T}$, leads to a ‘subgap’ feature in $\sigma(\omega)$ at finite T . Due to the large DOS at the gap edge this contribution to $\sigma(\omega)$ is large at low ω . Disorder broadens the coherence peaks and makes this subgap ω dependence flatter.

Fig.4(b) shows the low frequency results for $\omega \lesssim 2\Delta_0$ at $T = 0.2T_c^0$. In this frequency range, $\sigma(\omega)$ decreases monotonically with decreasing frequency, forming a hard gap at a disorder dependent frequency $\omega_g(V)$. ω_g is lowest between $0.75V_c$ and V_c , which seems to match with the critical disorder $V_c(T)$ at this T , see Fig.1. We do not find any discernible subgap feature at this temperature. The thermal factor $e^{-\Delta/T} \sim e^{-4T_c^0/0.2T_c^0}$ is too small.

At $T = 0.7T_c^0$, Fig.4.(c), the cleaner samples do show an upturn reminiscent of MB theory. However, even here for $V \gtrsim 0.5V_c$ the low frequency peak is absent due to the disorder and temperature induced broadening of the coherence peak.

In Fig.4(d), we show the the low frequency optical weight $w_{opt}(V, T, \Omega) = \int_0^\Omega d\omega \sigma(\omega, V, T)$ with $\Omega = 0.2t$. We find that the maximum in $w_{opt}(V, T)$ at a given T occurs at a disorder $V_{max}(T)$ that tracks the critical disorder $V_c(T)$. The inset shows the low frequency single

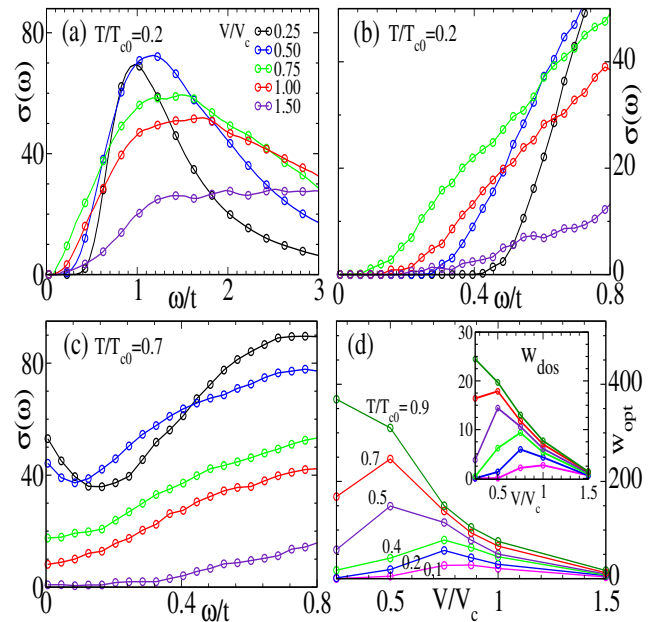


FIG. 4. Colour online: Optical conductivity and low frequency optical spectral weight. (a). The behaviour of $\sigma(\omega)$, measured in units of $\sigma_0 = \pi e^2/\hbar$, over a wide frequency range for disorder varying across the SIT. The temperature is $T = 0.2T_c^0$. (b). The low frequency behaviour of $\sigma(\omega)$ for varying V (same legends as in panel (a)), at $T = 0.2T_c^0$. (c). Same as in (b), now at $T = 0.7T_c^0$. Notice the absence of any gap, and the low frequency upturn, in samples with $V = 0.25V_c$ and $V = 0.5V_c$ which are still below their respective T_c . (d). Disorder dependence of the low frequency optical spectral weight, $w(V, \Omega)$, see text, at different T . Inset shows low frequency weight of the single particle spectrum.

particle weight $w_{dos}(V, T) = \int_0^{\Omega/2} d\omega N(\omega, V, T)$ and its strong correspondence with $w_{opt}(V, T)$. At $T = 0$ the behaviour of w_{dos} is consistent with earlier observation [17] that the gap is minimum close to V_c . The resulting maximum in w_{dos} persists, surprisingly, at finite T as well and also shows up in the behaviour of w_{opt} .

Since the weights are readily measurable, a qualitative explanation may be useful. Within our scheme the optical spectrum arises as a convolution over the single particle Greens function, so understanding $w_{dos}(V, T)$ can shed light on w_{opt} as well. Fig.3(d) provides a hint, where, crudely, $N(0, V, T)$ rises from zero at $T \ll T_c$ to its high T asymptote, $N_\infty(V)$, say, across T_c . $N_\infty(V)$ reduces monotonically with V . If we ignore the ‘width’ δT of the low to high temperature transition, then $N(0, V, T) \approx 0$ for $T < T_c(V)$ and $N(0, V, T) = N_\infty(V) \propto f_{SC}(V)$, the superconducting fraction, for $T > T_c$. If we approximate $w_{dos} \propto N(0)$, then at a given $T < T_c^0$, the $V < V_c(T)$ samples have $w_{dos} \sim 0$, and the $V > V_c(T)$ samples have $w_{dos} \sim N_\infty(V)$, with $dN_\infty(V)/dV < 0$. The peak would be obviously at $V \sim V_c(T)$. The real V dependence is of course smoother than the crude argument above suggests.

This observation ties together *independent measurements* on density of states, optical weight, and the spatial character of the superconducting state over the complete disorder-temperature window.

Discussion: In what follows we discuss the microscopic basis of our results, the limitations of our approach, and the connection of our results to experimental data.

(i) *Microscopic origin:* Within our approach the thermal properties are controlled by the mean value and thermal fluctuations of the pairing field Δ_i and the ‘density’ field ϕ_i . Disorder creates inhomogeneities in n_i which are fed back via the Hartree shift ϕ_i leading to an amplified effective disorder $V_{eff}^i = \epsilon_i + \phi_i$. Transport and spectral features are determined by the combined effect of V_{eff}^i and scattering from the Δ_i . **(a).** At weak disorder, $V \lesssim 0.25V_c$, the ground state has almost homogeneous n_i and $|\Delta_i|$, with perfect phase correlation. With increasing T , the $\langle |\Delta_i| \rangle$ increase and the θ_i randomise. The growing amplitude and phase disorder lead to increased scattering and $d\rho/dT > 0$ for $T > T_c$. The n_i remain roughly homogeneous over the relevant T window and the potential scattering just adds a constant contribution to the overall resistivity. **(b).** At intermediate disorder, $0.25V_c \lesssim V \lesssim 0.75V_c$, n_i is noticeably inhomogeneous in the ground state, leading to a large V_{eff}^i , but homogenize with increasing T . The $|\Delta_i|$, on the other hand, grow with increasing T in the high temperature regime. The result is a crossover in the resistivity with increasing T , with the $T \gtrsim T_c$ region showing $d\rho/dT < 0$ due to weakening V_{eff}^i , and the $T \gg T_c$ region showing $d\rho/dT > 0$ due to growing scattering from the Δ_i . A prominent pseudogap starts to form below $T_{corr} \lesssim T_c^0$, where strong local correlations appear among Δ_i , and deepens with decreasing T until T_c , where the bulk superconducting transition takes place and a hard gap is formed. **(c).** At large disorder, $V \gtrsim 0.75V_c$, the n_i inhomogeneity is very large in the ground state and SC clusters form only in ‘favourable’ regions [27] of this landscape. The insulating regions have a larger effective gap than the SC clusters. The n_i inhomogeneity, and the large V_{eff}^i survives to $T \gg T_c$ and leads to the activated resistivity.

(ii) *Limitations of our method:* There are two sources of error in our approach. **(a).** The static approximation: the auxiliary fields are in principle time dependent and their temporal (quantum) fluctuations can be significant in the vicinity of the $T = 0$ SIT. More concretely, as the electronic DOS becomes gapped due to pair formation, the dynamics of these bosonic pairs would play a significant role in transport and low frequency optics. This has been emphasized in a very recent preprint [29]. However, for the $U/t = 2$ that we have used, Fig.1 shows that the finite temperature SIT, for $V \lesssim 0.75V_c$, occurs in the presence of a finite DOS at the fermi level. So, at weak to moderate coupling, and for the finite temper-

ature SIT, our approach should be useful. **(b).** System size: weaker coupling, $U/t \lesssim 1$, is relevant experimentally, but difficult to access with current size limitations since the coherence length grows as $1/\Delta_0$. Our system size, $\sim 24 \times 24$, is significantly larger than what is accessible within QMC but still much smaller than the inhomogeneity scales observed experimentally. As a result, some of the predictions we make are only of qualitative value in the experimental context. We discuss these next.

(iii) *Comparison to experiments:* When comparing with experiments, it must be kept in mind that $U = 2t$ is already beyond the weak coupling BCS regime, with $2\Delta/kT_c^0 \sim 8$ instead of 3.5. Most real materials, explored in the SIT context are however in the BCS window, so the relevant $U_{eff}/t \lesssim 1$. This is also borne out by the rather low $T_c^0 \sim 10K$ of these materials [5, 6]. For the different indicators that we have calculated, a comparison to experiments reveal the following: **(a).** Resistivity: While our observation of a metal to insulator crossover in the normal state transport is consistent with experiments, experimental resistivities are less insulating than we observe [6, 11, 12]. For instance, at $V = 0.75V_c$, with $T_c = 0.4T_c^0$, our resistivity already shows insulating behaviour, falling to one-fourth of its maximum value by $T = 3T_c^0$, while the two dimensional TiN₃ sample in [5] only falls to 60% of its maximum value even though $T_c \sim 0.1T_c^0$ for that sample. Similar behaviour is seen in three dimensional NbN samples [6]. **(b).** Density of states: Pseudogap effects are more pronounced in our case, extending to larger temperatures. For instance, at $V = 0.5V_c$, this scale is around $T = 2.5T_c^0$, and by $V = V_c$, it extends beyond $T = 4T_c^0$. In contrast, experiments on three dimensional systems [6] indicate that the pseudogap vanishes at a temperature T^* that decreases initially with increasing disorder, and finally becomes constant at $T^* \sim 0.5T_c^0$ at large disorder. Two dimensional systems [3], on the other hand, do seem to show a qualitatively similar increase as ours, though their relevant scales are much smaller (for instance at $T_c = 0.1T_c^0$, $T^* \sim 1.4T_c^0$, whereas our scale is greater than $4T_c^0$.) **(c).** Optics: Low frequency features are sharply depressed, at low T , in our model at large disorder, whereas there is a much more modest effect in experiments [15, 16]. **(d).** Spatial character: Our results for local indicators reveal significant similarity, but also points of difference, in terms of spatial dependence and thermal variation, with recent experiments [9]. They will be dealt with in a separate publication [27].

Conclusion: We have studied the transport and spectral characteristics of a disordered s-wave superconductor over the complete disorder and temperature window relevant for the superconductor-insulator transition. We have identified the metal to insulator crossover in the normal state with increasing disorder and demonstrate a disorder window where the superconductor arises out of a high temperature ‘insulating’ state. We map out

the disorder and temperature dependence of the single particle and optical spectra, discover that their low frequency weight is non monotonic with disorder, and relate the weight to the superconducting spatial fraction in the disordered ground state.

Acknowledgments: We acknowledge use of the High Performance Computing Cluster at HRI. PM acknowledges support from a DAE-SRC Outstanding Research Investigator Award. We thank Amit Ghosal and Pratap Raychaudhuri for discussions.

-
- [1] P. W. Anderson, *J. Phys. Chem. Solids* **11**, 26 (1959).
- [2] For reviews, see A. M. Goldman and N. Markovic, *Phys. Today* **51**, No 11, 39 (1998), V. F. Gantmakher and V. T. Dolgoplov, *Phys. Usp.* **53**, 3-53 (2010), M. Sadoyskii, *Phys. Rep.* **282**, 225 (1997), D. Belitz and T. Kirkpatrick, *Rev. Mod. Phys.* **66**, 261 (1994).
- [3] B. Sacepe, *et al.*, *Nature Commun.* **1**, 140 (2010).
- [4] B. Sacepe, *et al.*, *Nature Phys.* **7**, 239 (2011).
- [5] B. Sacepe, *et al.*, *Phys. Rev. Lett.* **101**, 157006 (2008).
- [6] M. Chand, *et al.*, *Phys. Rev. B* **85**, 014508 (2012).
- [7] S. P. Chockalingam, *et al.* *Phys. Rev. B* **77**, 214503 (2008), S. P. Chockalingam, *et al.* *Phys. Rev. B* **79**, 094509 (2009)
- [8] M. Mondal, *et al.*, *Phys. Rev. Lett.* **106**, 047001 (2011).
- [9] A. Kamlapure, *et al.*, arXiv:1308.2880.
- [10] Y. Noat, *et al.*, arXiv:1205.3408.
- [11] M.A. Steiner, N.P. Breznay, A. Kapitulnik, *Phys. Rev. B* **77** 212501 (2008).
- [12] T.I. Baturina, *et al.*, *Phys. Rev. Lett.* **98** 127003 (2007).
- [13] T. I. Baturina, *et al.*, *Phys. Rev. Lett.* **99**, 257003 (2007).
- [14] V. Yu. Butko, P.W. Adams, *Nature* **409** 161 (2001).
- [15] M. Mondal, *et al.*, *Scientific Reports* **3**, 1357 (2013).
- [16] R.W. Crane, *et al.*, arXiv:cond-mat/0604107v3.
- [17] A. Ghoshal, M. Randeria and N. Trivedi, *Phys. Rev. Lett.* **81**, 3940 (1998), A. Ghoshal, M. Randeria and N. Trivedi, *Phys. Rev. B* **65**, 014501 (2001).
- [18] C. Huscroft and R.T. Scalettar, *Phys. Rev. Lett.* **81**, 2775 (1998).
- [19] R. Scalettar, N. Trivedi and C. Huscroft, *Phys. Rev. B* **59**, 4364 (1999).
- [20] K. Bouadim, *et al.*, *Nat. Phys.* **7**, 884 (2011).
- [21] *Condensed Matter Field Theory*, A. Altland and B. D. Simons, Cambridge University Press, (2010).
- [22] A. Erez and Y. Meir, *Europhys. Lett.* **91**, 47003 (2010).
- [23] Y. Dubi, *et al.*, *Nature*, **449**, 876 (2007).
- [24] M. Mayr, *et al.*, *Phys. Rev. Lett.* **94**, 217001 (2005).
- [25] S. Kumar and P. Majumdar, *Eur. Phys. J. B*, **50**, 571 (2006).
- [26] T. Paiva, *et al.*, *Phys. Rev. Lett.* **104**, 066406 (2010).
- [27] S. Tarat and P. Majumdar, to be published.
- [28] D. C. Mattis and J. Bardeen, *Phys. Rev.*, **111**, 412 (1958).
- [29] M. Swanson, Y. Lee Loh, M. Randeria, N. Trivedi, arXiv:1310.1073.